The Astrophysical Journal, 649:332–344, 2006 September 20

A *SPITZER SPACE TELESCOPE* STUDY OF SN 2002hh: AN INFRARED ECHO FROM A TYPE IIP SUPERNOVA

W. P. S. Meikle,[1] S. Mattila,[2] C. L. Gerardy,[1] R. Kotak,[3] M. Pozzo,[1] S. D. van Dyk,[4] D. Farrah,[5] R. A. Fesen,[6] A. V. Filippenko,[7] C. Fransson,[8] P. Lundqvist,[8] J. Sollerman,[9] and J. C. Wheeler[10]

Received 2006 April 11; accepted 2006 May 22

ABSTRACT

We present late-time (590–994 days) mid-IR photometry of the normal but highly reddened Type IIP supernova SN 2002hh. Bright, cool, slowly fading emission is detected from the direction of the supernova. Most of this flux appears not to be driven by the supernova event but instead probably originates in a cool, obscured star formation region or molecular cloud along the line of sight. We also show, however, that the declining component of the flux is consistent with an SN-powered IR echo from a dusty progenitor CSM. Mid-IR emission could also be coming from newly condensed dust and/or an ejecta/CSM impact, but their contributions are likely to be small. For the case of a CSM-IR echo, we infer a dust mass of as little as 0.036 $M_{\odot}$ with a corresponding CSM mass of $3.6(0.01/r_{\rm dg})\ M_{\odot}$, where $r_{\rm dg}$ is the dust-to-gas mass ratio. Such a CSM would have resulted from episodic mass loss whose rate declined significantly about 28,000 years ago. Alternatively, an IR echo from a surrounding, dense, dusty molecular cloud might also have been responsible for the fading component. Either way, this is the first time that an IR echo has been clearly identified in a Type IIP supernova. We find no evidence for or against the proposal that Type IIP supernovae produce large amounts of dust via grain condensation in the ejecta. However, within the CSM-IR echo scenario, the mass of dust derived implies that the *progenitors* of the most common of core-collapse supernovae may make an important contribution to the universal dust content.

Subject headings: supernovae: general — supernovae: individual (NGC 6946, SN 2002hh)

1. INTRODUCTION

A major goal in the study of core-collapse supernovae (CCSNe) is to test the proposal that they are, or have been, a significant source of dust in the universe. The physical conditions believed to prevail in the expanding SN ejecta make this an attractive idea. Large abundances of suitable refractory elements are present. Cooling by adiabatic expansion and molecular emission takes place. Dynamical instabilities can produce density enhancements or "clumping." Support for these ideas is provided by isotopic anomalies in meteorites that indicate that some grains must have formed in CCSNe (Clayton et al. 1997). Interest in CCSNe as dust producers has increased recently due to the problem of accounting for the presence of dust at high redshifts (Fall et al. 1989, 1996; Pei et al. 1991; Pettini et al. 1997; Bertoldi et al. 2003). In these early eras, much less dust production from novae and asymptotic giant branch (AGB) stars is expected since fewer stars will have evolved past the main-sequence phase. Consequently, supernovae arising from Population III stars are proposed as the main early-universe source of dust. Models of dust formation in supernovae (Todini & Ferrara 2001; Nozawa et al. 2003) succeed in producing copious amounts of dust—around 0.1–1 $M_{\odot}$ even in the low-metallicity environments at high redshifts. This is enough to make supernovae a major contributor to the dust content of the universe.

Observations of SN 1987A yielded indirect evidence that large masses of dust can be produced in CCSNe. Around 500 days post-explosion, its UVOIR light curve dipped below the radioactive deposition input (Whitelock et al. 1989). At the same time, the mid-IR flux increased, nicely accounting for the UVOIR deficit (Whitelock et al. 1989 and references therein). This suggests substantial dust formation in the ejecta, although the actual mass involved is uncertain. Spectroscopic observations of SN 1987A (Danziger et al. 1991; Dwek et al. 1992; Spyromilio & Graham 1992) indicate that, at 600–700 days, most of the silicon and iron emission disappeared from the optical/near-IR wavelength range. If we attribute this loss to depletion onto grains (e.g., Mg_2SiO_4, $MgSiO_3$, Fe_3O_4), then this implies a large mass of dust—perhaps as much as 0.1 $M_{\odot}$. However, it may be that cooling and expansion to below the critical density can account for much of the fading of the spectral lines (Fransson & Chevalier 1987; Lucy et al. 1991; Meikle et al. 1993).

In spite of the SN-grain condensation hypothesis being over 30 years old (Cernuschi et al. 1967; Hoyle & Wickramasinghe 1970) there is still no *direct* observational evidence that SNe are major dust sources. In particular, it is not known if ordinary Type IIP SNe produce large amounts of dust. Dust condensation in CCSN ejecta can be observed directly in two ways. The first method makes use of the attenuating effect on the red wings of the broad ejecta lines during the nebular phase. This technique

[1] Astrophysics Group, Blackett Laboratory, Imperial College London, Prince Consort Road, London SW7 2AZ, UK; p.meikle@imperial.ac.uk, c.gerardy@imperial.ac.uk, m.pozzo@imperial.ac.uk.
[2] Department of Physics and Astronomy, Queen's University Belfast, County Antrim BT7 1NN, UK; s.mattila@qub.ac.uk.
[3] European Southern Observatory, Karl-Schwarzschild-Strasse 2, D-85748 Garching bei München, Germany; rkotak@eso.org.
[4] Infrared Processing and Analysis Center, California Institute of Technology, Mail Code 100-22, 770 South Wilson Avenue, Pasadena, CA 91125; vandyk@ipac.caltech.edu.
[5] Department of Astronomy, 106 Space Sciences Building, Cornell University, Ithaca, NY 14853; duncan@isc.astro.cornell.edu.
[6] Department of Physics and Astronomy, Dartmouth College, 6127 Wilder Laboratory, Hanover, NH 03755-3528; fesen@snr.dartmouth.edu.
[7] Department of Astronomy, 601 Campbell Hall, University of California, Berkeley, CA 94720-3411; alex@astro.berkeley.edu.
[8] Stockholm University, AlbaNova University Center, Stockholm Observatory, Department of Astronomy, SE-106 91 Stockholm, Sweden; claes@astro.su.se, peter@astro.su.se.
[9] Dark Cosmology Centre, Niels Bohr Institute, University of Copenhagen, Juliane Maries Vej 30, 2100 Copenhagen, Denmark; jesper@astro.ku.dk.
[10] University of Texas at Austin, Department of Astronomy, Austin, TX 78712; wheel@astro.as.utexas.edu.

has the advantage of being relatively unambiguous in its ability to demonstrate the presence of new dust, although extraction of quantitative information about the quantity and nature of the grains may be more difficult. The method is technically challenging in that it requires high S/N, high spectral resolution observations taken at as much as 2 years post-explosion. Consequently, prior to SN 2002hh only three CCSNe—the Type IIpec SN 1987A (Danziger et al. 1991), the Type IIn SN 1998S (Pozzo et al. 2004), and the Type IIP SN 1999em (Elmhamdi et al. 2003)—had been studied in this way. In all three cases, dust masses of just 10^{-4} to 10^{-3} $M_\odot$ were found to be adequate to account for the attenuation, although the actual mass of dust could be larger. In SNe 1987A and 1998S, variation of the strength of the attenuation from optical to NIR wavelengths was much weaker than would be expected from an optically thin screen of small grains. Thus, either the grain size was remarkably large (>5 μm radius) or the grains existed in optically thick clumps. The former explanation is unlikely since such large grains are not produced in grain condensation models (Todini & Ferrara 2001). On the other hand, as mentioned above, clumping due to dynamical instabilities is quite plausible. The mass of dust may also have been underestimated if not all of it is "backlit" by spectral line emission. The Elmhamdi et al. (2003) result for SN 1999em is of special importance since this supernova was a normal Type IIP event. Prior to the launch of the *Spitzer Space Telescope* (*Spitzer*), this stood as the only direct observational evidence of dust formation in a typical CCSN.

The other way of directly studying newly condensed dust is by means of thermal IR emission from the grains. Thirteen CCSNe have exhibited late-time NIR excesses (Gerardy et al. 2002 and references therein). (Note that the peculiar Type Ia SN 2002ic has also shown a strong IR excess [Kotak et al. 2004].) This is attributed to thermal emission from hot grains. Curiously, 12 of the CCSNe were not of Type IIP, while for the 13th, SN 1982L, the subtype is unknown. Moreover, it cannot be assumed that the NIR excess was due to emission from newly formed grains. An alternative mechanism is thermal emission from preexisting dust in the progenitor wind, heated by the supernova peak luminosity—the so-called IR echo. Heating of circumstellar material (CSM) dust by ejecta/shock interaction is another possibility. Prior to the launch of *Spitzer*, only for SNe 1987A and 1998S had persuasive IR-excess–based evidence for dust condensation during an observed supernova explosion been put forward (Lucy et al. 1991; Dwek et al. 1992; Meikle et al. 1993; Roche et al. 1993; Wooden et al. 1993; Pozzo et al. 2004). In both objects it was found that a dust mass of only $\sim 10^{-3}$ $M_\odot$ was sufficient to account for the observed IR flux, although a considerably larger mass could have been concealed in optically thick clumps. Mid-IR studies of the supernova remnant Cassiopeia A (Dwek et al. 1987; Lagage et al. 1996; Douvion et al. 2001) indicate that dust formation took place during its explosion, but again the mass of directly observed dust is small. The claim by Dunne et al. (2003) that at least 2 $M_\odot$ of dust formed in the Cas A supernova has been contested by Dwek (2004) and Krause et al. (2004).

The availability of *Spitzer* has provided an excellent opportunity for us to test the dust-condensation hypothesis in a statistically significant number of typical supernovae. It provides high-sensitivity imaging over the mid-IR covering the likely peak of the dust thermal emission spectrum. This can provide a superior measure of the total flux, temperature, and, possibly, dust emissivity than can be achieved at shorter wavelengths. Moreover, the longer wavelength coverage of *Spitzer* lets us detect cooler grains and see more deeply into dust clumps than was previously possible for typical nearby CCSNe. In addition, multiepoch observations with *Spitzer* may allow us to distinguish between dust condensation and IR echoes via the light-curve shape; for example, a flat-topped light curve favors an IR echo (e.g., Dwek 1983).

SN 2002hh was discovered in NGC 6946 on UT 2002 October 31.1 (Li 2002). The supernova was not detected on a KAIT image on October 26.1 at a limiting magnitude of $\sim$19.0. We therefore adopt 2002 October 29 $\pm$ 2 (JD 2,452,577 $\pm$ 2) as the explosion epoch. NGC 6946 is at a distance of 5.9 Mpc (Karachentsev et al. 2000) and has produced seven other SNe. From optical spectra taken on 2002 November 2 Filippenko et al. (2002) identified SN 2002hh as a young, highly reddened Type II supernova. It peaked at $V \sim 17.2$ on 2002 November 5. A detailed study of the optical and near-IR evolution of SN 2002hh during its first year has been presented by Pozzo et al. (2006). Their light curves show SN 2002hh to have been a Type IIP event. Using JK_s images taken on 2002 Nov. 18.86, Meikle et al. (2002) inferred a host-galaxy extinction of $A_V \sim 5.0$. This was confirmed by Pozzo et al. (2006), who propose a two-component extinction law to account for the spectral reddening and the depth of K I interstellar absorption.

Stockdale et al. (2002) detected radio emission at 8.435 and 22.485 GHz at 17 days. They suggested that "the apparently optically thin character of the radio emission, if confirmed, may indicate that the circumstellar interaction is weak and is evolving unusually rapidly." SN 2002hh was also detected at 1396.75 MHz by Chandra et al. (2003) at 59 days. Pooley & Lewin (2002) detected X-ray emission at 27 days. They state that the rather hard, highly absorbed spectrum is as might be expected given the high reddening, and that the low luminosity supports the radio indication that little circumstellar interaction was taking place at that time. Chevalier et al. (2006) find that an optical depth of unity occurred at day 62 at 1.4 GHz, implying a mass-loss rate of $7 \times 10^{-6}(T_{\rm cs}/10^5\ {\rm K})^{3/4} v_{w1}\ M_\odot\ {\rm yr}^{-1}$, where $T_{\rm cs}$ is the temperature of the CSM and v_{w1} is the progenitor wind velocity in units of 10 km s^{-1}. Beswick et al. (2005) measured radio emission at 4.860 GHz at 381 days, and at 1.425 GHz at 899 days. Late-time mid-IR observations have been reported by Barlow et al. (2005), and these are discussed below.

Here we present results of *Spitzer* observations of SN 2002hh. This forms part of the work of our Mid-Infrared Supernova Consortium (MISC), which is using *Spitzer* to observe a substantial sample of nearby SNe of all types and over a wide range of epochs. Preliminary results from our SN 2002hh *Spitzer* observations have been presented by Meikle (2005).

2. OBSERVATIONS

SN 2002hh was observed with the Infrared Array Camera (IRAC; Fazio et al. 2004) on *Spitzer* in all four channels (3.6, 4.5, 5.8, and 8.0 μm) and at four epochs spanning 590–994 days postexplosion. The observation log is given in Table 1. As part of our *Spitzer* supernova programs (PID:3248, 20256) the supernova was observed at epochs 684, 758, and 994 days. For each filter, a full-array 20-point medium dither was used. The integration time per frame was 26.8 s, which kept the counts per frame on the target at well below the nonlinearity limit. Thus, the total integration time per channel at a given epoch was 536 s. The target was also observed serendipitously within the *Spitzer* Infrared Nearby Galaxies Survey (SINGS; Kennicutt et al. 2003) at epochs 590 and 758 days. In this case, for each filter a mapping scheme in high–dynamic-range mode was used. The total integration time per channel at a given epoch was 214 s. All the data were reprocessed in the S11.0.2 pipeline. We use the post-basic calibrated data (PBCD) product throughout. From the point of view of dust condensation, the epochs covered are particularly interesting

TABLE 1
Log of Mid-IR (IRAC) Observations of SN 2002hh with *Spitzer*

JD (2,453,000+)	Date (UT)	Epoch[a] (days)	t_{int}[b] (s)	Program
167.3.....	2004 Jun 10.8	590	214	SINGS
260.8.....	2004 Sep 12.3	684	536	MISC
335.2.....	2004 Nov 25.7	758	214	SINGS
335.3.....	2004 Nov 25.8	758	536	MISC
571.7.....	2005 Jul 20.2	994	536	MISC

[a] Days after explosion (JD −2,452,577).
[b] Integration time per filter.

since, in the case of SN 1987A, the mid-IR luminosity from the ejecta dust peaked around 600 days (Bouchet & Danziger 1993).

3. RESULTS

In Figure 1 we show *Spitzer* (IRAC) 8 μm images ($200'' \times 200''$ sections) of the SN 2002hh field taken at the earliest and latest epochs, viz., 590 days (*left-hand panel*) and 994 days (*center panel*). The supernova is located within a complex distribution of sources forming part of the spiral arm structure of NGC 6946. The field is dominated by a bright star lying about $9''$ from the supernova at a position angle (P.A.) of 298°. The star's magnitudes are $B = 16.1$, $V = 15.2$ (NED). This star is also recorded in the Two Micron All Sky Survey (2MASS) catalog as J20344320+6007234, with magnitudes $J = 15.9$, $H = 15.5$, and $K = 15.3$. (Henceforth, the star will be referred to as the "2MASS star.") Extended emission lies between the 2MASS star and the supernova location. We note that there is little apparent difference between the images from one epoch to the next. The other three channels show a similar lack of change. However, the right-hand image shows the effect of subtracting the 994 day image from the 590 day one (details below). A bright point source is apparent at the supernova location. This indicates the presence of a declining source, and we suggest below that the supernova is the cause of this. The contribution that the supernova makes to the total flux from this location is also discussed below.

To illustrate the complexity of the SN 2002hh field, in Figure 2 we compare the 590 day 8 μm image with the same field at a number of other wavelengths and epochs. In a *K*-band 266 day image obtained at the IRTF (Pozzo et al. 2006) the supernova is clearly present. A preexplosion *B*-band image (Larsen & Richtler 1999) indicates a dark dust-lane close to the supernova location, while a preexplosion Hα image (Knapen et al. 2004) reveals emission that extends from the 2MASS star almost to the SN position.

Aperture photometry of the supernova was carried out on the PBCD data, using the Starlink package GAIA (Draper et al. 2004). The brightness and complexity of the sources in the supernova field, together with the IRAC spatial resolution of FWHM $\sim 2''$ (at 8.0 μm), makes the extraction of reliable photometry quite challenging. We performed simple aperture photometry on three different forms of the data, viz., (1) original images, (2) all images aligned to the same orientation and position, and (3) PSF-matched, intensity-matched, subtracted images. A circular aperture of radius $3\farcs3$ (2.7 pixels) was used for the photometry. This is sufficiently large to encompass the flux out to beyond the first Airy ring in the longest wavelength band (8.0 μm), thus reducing the size of aperture correction needed in the final flux determination. The aperture radius corresponds to a distance of $\sim$100 pc at SN 2002hh. A larger aperture was not used in order to minimize contamination from the 2MASS star. For each measurement, the aperture was centered to within $\pm 0\farcs1$ (0.08 pixels) of the supernova position as reported by Li (2002) and given in the NED and SIMBAD databases. To test the accuracy of our positioning procedure, we measured the world coordinate system (WCS) coordinates of the centroid of isolated field stars for all the images. The dispersion in the 3.6 and 4.5 μm images was found to be $0\farcs18$ in both axes. For the 5.8 and 8 μm images the dispersion was $0\farcs34$. We note that the radio position of SN 2002hh reported by Stockdale et al. (2002) differs from that given by Li (2002) by $0\farcs5$, or about 0.4 of an IRAC pixel. We checked the effect of centering on the Stockdale et al. position and found that it increased the measured fluxes by just 1%–6%. Aperture correction factors were applied as specified in Table 5.7 of the IRAC Data Handbook (Reach et al. 2006). For the unsubtracted images, the sky was measured using a clipped mean sky estimator and concentric annuli with radii chosen to avoid background sources as far as possible. Measurements were obtained for two annulus settings, viz., inner/outer radius values of 4/5 and 7/8 times the aperture radius, respectively, and the mean flux value was adopted for each channel/epoch. For the 758 day flux, the mean of the SINGS and MISC data was adopted. The error contribution caused by position uncertainty was estimated by offsetting the aperture by an amount equal to the position uncertainty (dispersion) described above and remeasuring the flux. This was carried out for a number of directions from the WCS coordinates of the supernova.

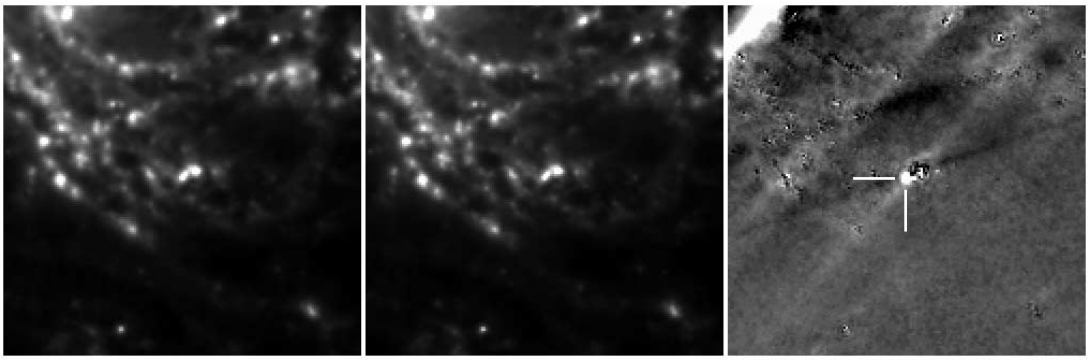

Fig. 1.—*Left, center:* IRAC 8 μm images ($200'' \times 200''$ sections) of the SN 2002hh field taken at 590 and 994 d postexplosion, respectively. North is up, and east is to the left. The center of the field is dominated by a bright 2MASS star. Extended emission to the approximate southeast of the star is also apparent. There appears to be little difference in the flux at the supernova position between the two images. *Right:* Subtraction of the center image (994 days) from the left-hand image (590 days) after PSF and intensity matching. The supernova, indicated by the tick marks, is clearly visible.

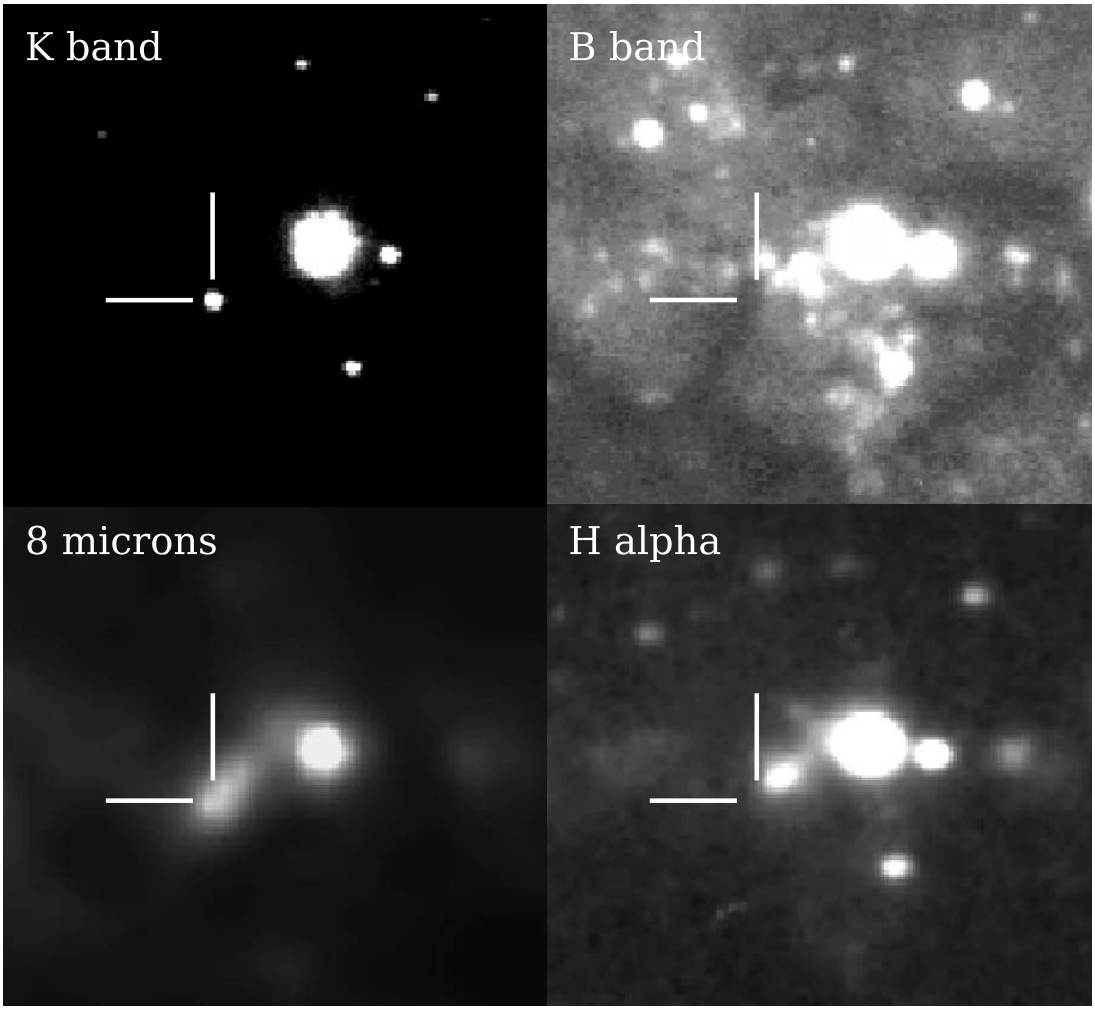

FIG. 2.—SN 2002hh field viewed at a variety of wavelengths and epochs. The FOV of each image is $38'' \times 35''$. North is up, and east is to the left. All the images have been aligned (including rebinning, rotation, and shifting) to the Hα image. The SN location is marked with ticks in each image based on the coordinates measured from the *K*-band image. In each image, the bright 2MASS star lies about $9''$ and P.A. 298° from the supernova location. The *K*-band image of SN 2002hh was obtained with SPEX at the IRTF at 266 days (Pozzo et al. 2006), and the 8 μm *Spitzer* (IRAC) image was acquired at 590 days. The preexplosion *B*-band image is from Larsen & Richtler (1999). Note the dust lane close to the supernova position. The preexplosion Hα image is from Knapen et al. (2004). It illustrates the extended H II region close to the supernova position.

Aperture photometry of the supernova region using the original unaligned, unsubtracted images reveals only a hint of temporal variation between 590 and 994 days (Table 2). While the flux at 3.6 μm exhibits an increase of about 0.2 mJy, declines of about 0.2, 1, and 3 mJy appear to have occurred at 4.5, 5.8, and 8.0 μm, respectively, i.e., a fall of 10%–15% over a period of $\sim$400 days. We found that the absolute flux values could be influenced by the precise choice and placement of the aperture. Suspecting that part of the dispersion in values arose from the effects of aperture placement uncertainty on randomly orientated images, we then aligned all the images to the same orientation and repeated the aperture photometry. The alignment procedure comprised rotation and *x*, *y* shifts, making use of the four or five most compact isolated sources near the SN, per frame. This resulted in rms values between $0''.02$ and $0''.08$ for the alignment solutions. The 590, 684, and 758 day data were aligned to the 994 day data. The results of the photometry of the supernova region using these aligned, unsubtracted images are given in Table 3

TABLE 2
MID-IR FLUXES OF THE SN 2002hh REGION: UNALIGNED, UNSUBTRACTED IMAGES

EPOCH (days)	FLUX (mJy)			
	3.6 μm	4.5 μm	5.8 μm	8.0 μm
590.....	1.78(0.06)[a]	1.78(0.04)	6.51(0.28)	21.5(0.9)
684.....	1.90(0.06)	1.81(0.04)	5.57(0.28)	19.2(0.9)
758.....	2.13(0.06)	1.60(0.04)	5.24(0.28)	21.0(0.9)
994.....	2.00(0.06)	1.57(0.04)	5.31(0.28)	18.0(0.9)

[a] Errors are shown in parentheses.

TABLE 3
MID-IR FLUXES OF THE SN 2002hh REGION: ALIGNED, UNSUBTRACTED IMAGES

EPOCH (days)	FLUX (mJy)			
	3.6 μm	4.5 μm	5.8 μm	8.0 μm
590.....	1.76(0.05)[a]	1.72(0.04)	6.33(0.27)	21.3(0.8)
684.....	1.86(0.05)	1.74(0.04)	5.50(0.27)	19.0(0.8)
758.....	2.09(0.05)	1.58(0.04)	5.14(0.27)	20.8(0.8)
994.....	2.00(0.05)	1.57(0.04)	5.16(0.27)	17.8(0.8)

[a] Errors are shown in parentheses.

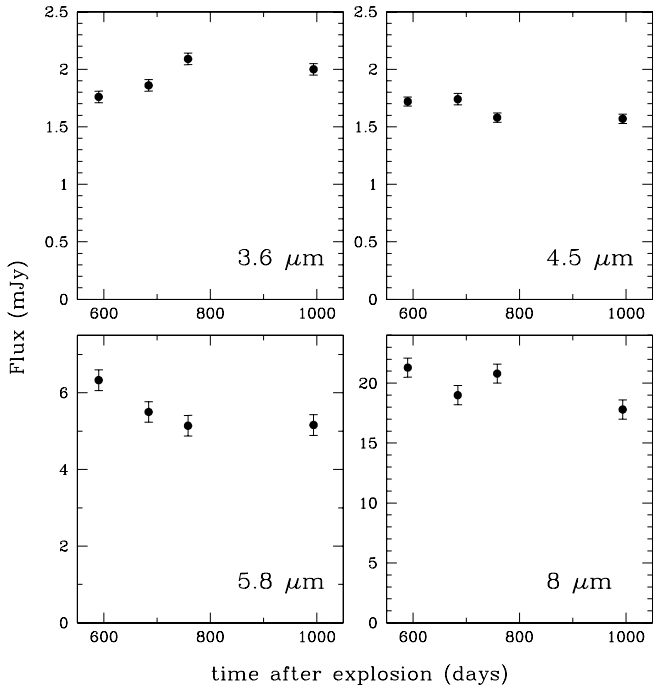

FIG. 3.—Mid-IR photometry of the SN 2002hh region using a 6.″5 diameter aperture centered at the supernova position in aligned, unsubtracted images.

and Figure 3. The photometric errors are slightly reduced relative to those for the unaligned images, but temporal trends in the four channels are much the same.

In our third approach, we aimed to achieve a more sensitive measure of any time-dependent behavior through the use of image matching and subtraction techniques as implemented in the ISIS 2.2 image subtraction package (cf. Alard & Lupton 1998; Alard 2000). To provide a better control of the image matching procedure, the original image subtraction code was first modified to allow the user to input the center coordinates for the regions used for matching the images (see also Mattila & Meikle 2001). We selected 12, $24'' \times 24''$ regions centered on some of the brightest and most pointlike sources within $120''$ of the supernova, avoiding any artifacts present in the backgrounds of the frames (the 2MASS star was not included due to its proximity to the SN). We employed no background variability for the backgrounds between the frames, and order 0, 1, and 2 variability for the convolution kernel. While the IRAC PSF is not expected to vary with time, the shifting and rotating procedures applied to the 590, 684, and 758 day data resulted in their PSFs being widened relative to those of the 994 day images. We therefore convolved the 994 day images to match each of the other epochs in turn. We found that the subtracted images showed a significantly lower level of residuals at the location of bright sources as we increased the order of spatial kernel variability from 0 to 1. This is because a spatially varying kernel is able to correct for small imperfections in the image alignment (Alard 2000). However, only a modest improvement was found going from order 1 to 2. We therefore made use of the order 1 variability for all the images. The 994 day images were then convolved with a $17'' \times 17''$ spatially varying kernel, and their intensities and backgrounds were matched with the aligned images. Finally, the matched 994 day reference image was subtracted from each aligned image to yield the difference in the SN flux between any given epoch and the reference image epoch. An example from the procedure is given in Figure 1, where we show the image subtraction of the 994 day 8.0 μm image from that at

TABLE 4

MID-IR FLUXES OF SN 2002hh: ALIGNED, SUBTRACTED IMAGES

EPOCH (days)	FLUX (mJy)[a]			
	3.6 μm	4.5 μm	5.8 μm	8.0 μm
590.....	<0.2	0.227(0.010)[b]	0.82(0.07)	2.30(0.09)
684.....	<0.2	0.241(0.013)	0.58(0.06)	1.69(0.16)
758.....	<0.2	0.09(0.07)	0.32(0.12)	1.66(0.04)

[a] The fluxes show the *change* in flux relative to the 994 day values.
[b] Errors are shown in parentheses.

590 days. A bright pointlike source is clearly visible in the subtracted image and, to within the uncertainty of the WCS coordinates, it lies at the supernova position. Comparison of the source FWHM with those of isolated stars confirms that it is indeed a point source. We conclude that the subtracted-image point source is entirely due to the supernova. The accuracy of the subtraction procedure is clear from the faintness of the residual emission in the field.

Aperture photometry of the supernova in the subtracted images was then carried out using the same aperture size and positioning as before. The subtraction procedure achieved a good match between the background levels of the two frames, yielding net background levels close to zero in the subtracted frames. Consequently, a bonus of using subtracted images was that no background annuli were needed in the photometry, thus reducing possible contamination by imperfectly subtracted sources lying within the annuli. The uncertainties in the photometry include the effects of photon statistics, aperture positioning error, and imperfections in the image matching procedure. To investigate the uncertainties introduced by image matching, we repeated the image matching and subtraction procedure using another set of regions (with some overlap with the first one) for fitting the convolution kernel and background. We also compared the subtraction results for the MISC and SINGS data on 758 days. From this we conclude that systematic uncertainties due to the image matching procedure dominate the errors in the supernova photometry. At 3.6 μm no significant change in flux between any epoch was detected at the level of $\sim$0.2 mJy (2 σ). This is in spite of a small apparent brightening seen in the unsubtracted image fluxes with a photometry error of just $\pm$0.05 mJy. We attribute the increased error in the 3.6 μm subtracted image photometry to a very strong residual from the 2MASS star produced during the subtraction process, possibly due to saturation in the vicinity of the star. However, in the other three channels, as hoped, the uncertainty was reduced relative to the unsubtracted image photometry. At 5.8 and 8.0 μm we see error reduction of factors of $\sim$3–8. The results are shown in Table 4 and Figure 4. The 4.5, 5.8, and 8.0 μm fluxes all exhibited small but significant changes from epoch to epoch. Between the first and last epochs, declines of about 10% are seen relative to the total flux. This confirms the suspected declines in the unsubtracted images. At 4.5 μm, there is little change between 758 and 994 days. We suspect that, by this epoch, the 4.5 μm flux had faded below detectability. However, at 5.8 and 8.0 μm there is no evidence to suggest that the observable decline had ceased by the last epoch (994 days). The likelihood of a subsequent decline is considered below in the context of the IR echo model.

The important conclusion that can be drawn from our demonstration of temporal variation in the mid-IR fluxes is that at least a small fraction of the total mid-IR flux from a region within $\sim$100 pc of SN 2002hh must have been powered by the supernova.

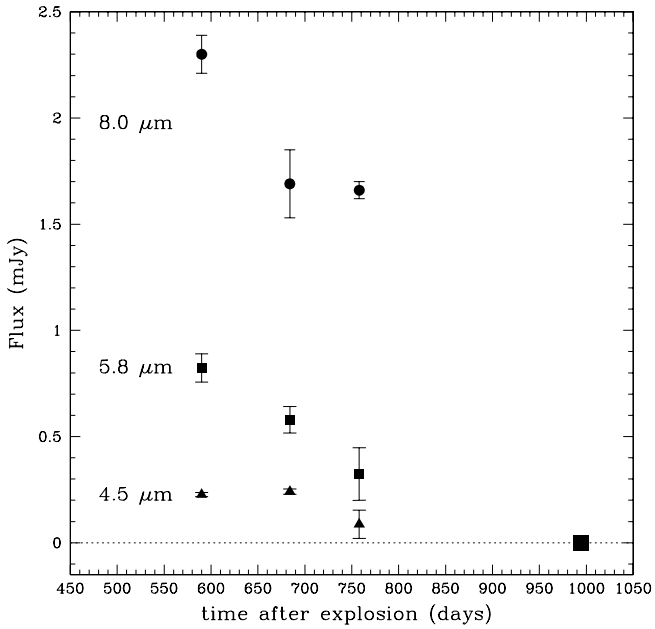

FIG. 4.—Mid-IR photometry of SN 2002hh using a 6″.5 diameter aperture centered at the supernova position in subtracted images (see text). The square point at zero flux represents the 994 day level for all four channels. The images at 994 days were subtracted from the corresponding channels at the other epochs.

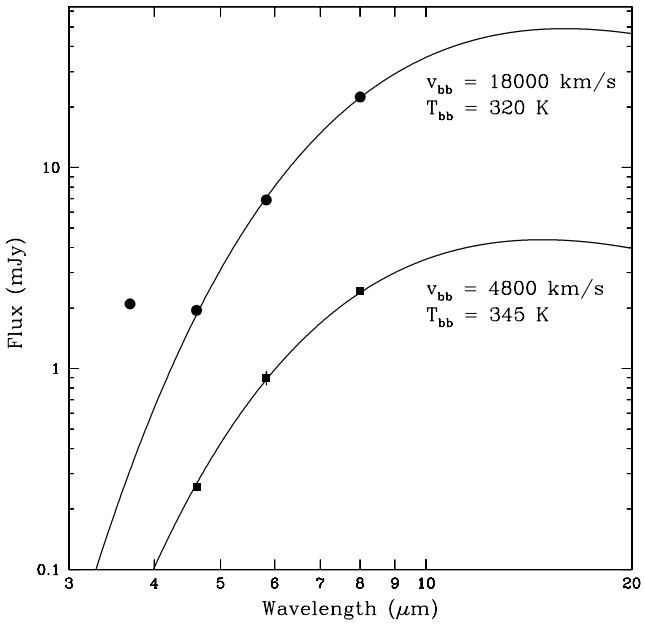

FIG. 5.—IRAC photometry of the SN 2002hh region using a 6″.5 diameter aperture centered at the supernova position. The filled circles show the fluxes obtained in the aligned, unsubtracted images at 590 days. The filled squares show the fluxes obtained in the subtracted images where the 994 day images have been subtracted from the 590 day images. Each point has been dereddened according to the two-component extinction of Pozzo et al. (2006), extrapolated to the mid-IR using the Cardelli et al. (1989) law. The individual points are located at the effective wavelengths of the IRAC filters for a 325 K blackbody. Also shown are blackbody spectra adjusted to match the 4.5, 5.8, and 8 μm points for both unsubtracted and subtracted cases.

In the following section we discuss what fraction of the total flux in the aperture might be reasonably attributed to the supernova, and what its cause might be.

4. ANALYSIS AND DISCUSSION

Interpretation of the mid-IR measurements of SN 2002hh depends critically on how much of the flux is actually from the supernova ejecta and/or nearby material, and how much is from causally unconnected line-of-sight sources in NGC 6946. In the following, we consider three possible supernova-driven sources, viz., newly condensed ejecta dust, an IR echo from surrounding dust, and an ejecta/dusty CSM interaction. Evidence of mid-IR emission from dust associated with SN 2002hh has been discussed by Barlow et al. (2005) and Meikle (2005).

4.1. *Mid-IR Emission from Newly Condensed Ejecta Dust*

In Figure 5 (*filled circles*) we plot the dereddened (see below) spectral energy distribution (SED) for the total flux in the aperture (unsubtracted, aligned images) for epoch 590 days. The SED is roughly flat between 3.6 and 4.5 μm but then rises swiftly toward longer wavelengths. This suggests a combination of two spectra. We suggest that the shorter wavelength emission is due to a combination of nebular emission from the ejecta plus residual stellar/nebular background (recall that the aperture radius is equivalent to $\sim$100 pc), while the longer wavelength component indicates something much cooler. The obvious candidate source is warm dust. We have explored this by matching blackbodies to the 4.5, 5.8, and 8.0 μm fluxes. In this procedure, the IRAC fluxes were first dereddened according to the two-component extinction of Pozzo et al. (2006) and then extrapolated to the mid-IR using the Cardelli et al. (1989) law. This yielded scaling factors of 1.191, 1.133, 1.089, and 1.053 for 3.6, 4.5, 5.8, and 8.0 μm, respectively. It might be argued that such an extrapolation to this wavelength region is unjustified. Draine (2003) gives a range of possible extinction laws in the mid-IR. In particular, the 8.0 μm extinction may be higher than the Cardelli et al. law extrapolation suggests, due to the 9.7 μm silicate absorption. However, on the basis of Figure 4 in Draine (2003) we estimate that other possible extinction laws would change the mantissae of the mid-IR dereddening factors by only about 10%–15%. Good matches to the dereddened fluxes are obtained with a temperature of 320 K at all epochs, and a blackbody radius of $\sim 9 \times 10^{16}$ cm at 590 days declining to $\sim 8 \times 10^{16}$ cm at 994 days. The blackbody match for 590 days is shown in Figure 5. For this blackbody to reach a radius of 9×10^{16} cm requires a velocity of 18,000 km s^{-1} after the supernova exploded. The formation of dust at this velocity is highly implausible. Such high velocities are generally only seen in the extreme outer zones of the H/He envelope. Furthermore, the extreme wings of the brightest, earliest, postplateau (epoch $\sim$150 days) metal lines in SN 2002hh correspond to velocities of no more than $\sim$4500 km s^{-1} (Pozzo et al. 2006). (We ignore the strong, broad calcium triplet P Cygni feature present in the 44 day spectrum. Given the intrinsic strength of the Ca triplet transition plus the fact that this epoch is less than halfway through the plateau phase, the feature is presumably caused by a small amount of preexplosion calcium in the progenitor atmosphere). We therefore rule out ejecta dust, whether heated by radioactivity or a reverse shock from a CSM impact, as the source of the total flux in the 3″.3 radius aperture. A similar argument against newly formed dust was made by Barlow et al. (2005) and Meikle (2005).

An additional argument against radioactively heated ejecta dust being the source of the total mid-IR flux in the aperture is provided by energy considerations. Integrating over the single-temperature blackbody matches, the total luminosity at 590 days is $\sim 6 \times 10^{40}$ ergs s^{-1}. SN 1987A produced a similar mass of ^{56}Ni to that seen in SN 2002hh (Pozzo et al. 2006). (We assume that the masses of other radioactive materials [e.g., ^{57}Ni] were also

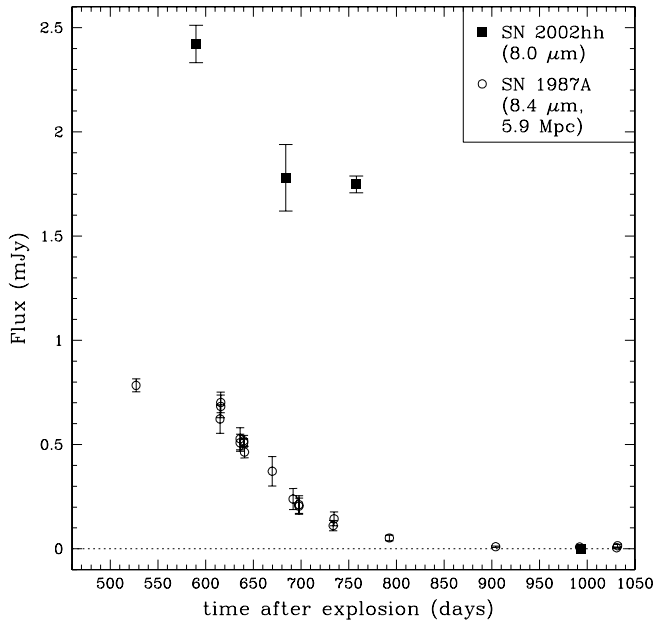

FIG. 6.—8.0 μm photometry (*filled squares*) of SN 2002hh using a 6.″5 diameter aperture centered at the supernova position in subtracted images. Each point has been dereddened according to the two-component extinction of Pozzo et al. (2006), extrapolated to the mid-IR using the Cardelli et al. (1989) law. The squares at zero flux represents the 994 day level. Also shown (*open circles*) is the dereddened 8.4 μm light curve of SN 1987A, shifted to the SN 2002hh distance of 5.9 Mpc.

similar between the two events.) Assuming a similar deposition fraction in SN 2002hh, at 590 days radioactive decay would deposit only $\sim 3 \times 10^{39}$ ergs s^{-1} in the ejecta (Li et al. 1993), falling to about 2% of this by 994 days.

While the above discussion rules out condensing dust as the source of the total IR flux in the aperture, emission from newly condensed grains might be responsible for the temporally varying component. In Figure 5 (*filled squares*) we also plot the SED for the supernova obtained from the subtracted images for epochs 590, 684, and 758 days. The lower flux in this case means that the blackbody radius is much reduced. Nevertheless, to obtain a good match we require a blackbody velocity of $\sim$4800 km s^{-1}, with temperatures of 345, 315, and 295 K for each epoch, respectively. Even this lower velocity slightly exceeds that of the fastest metals seen in the postplateau SN 2002hh spectra (see above). Moreover, the mass of dust required to create a blackbody at 8 μm lying at 4800 km s^{-1} is large. A simple calculation suggests that a mass of at least $\sim$0.005 $M_\odot$ would be needed (assuming a grain radius $\sim$0.1 μm, material density $\rho = 3$ g cm^{-3}, and absorption/emission efficiency $\propto \lambda^{-1}$). It seems unlikely that so much dust could form at such a high velocity.

As in the total IR flux case, an additional argument against radioactively heated ejecta dust being the source of the declining mid-IR flux in the aperture is provided by energy considerations. Assuming a similar deposition of radioactive decay energy in SNe 1987A (Li et al. 1993) and 2002hh (see above), by 758 days the radioactive decay deposition luminosity in SN 2002hh would be only 35% of the blackbody luminosity in the 0–10 μm range. Indeed, the luminosities of the subtracted-image SN 2002hh 0–10 μm integrated blackbody spectra are 3–5 times greater than the coeval thermal emission from condensing dust in SN 1987A (Wooden et al. 1993). Yet, as we have indicated, the masses of radioactive material in the two SNe appear to be similar. In Figure 6 we compare the subtracted-image 8.0 μm fluxes with the 8.4 μm light curve of SN 1987A, scaled to the SN 2002hh distance. The 8.4 μm emission from SN 1987A during this phase is generally accepted as being mainly from newly condensed dust in the ejecta. Between 550 and 1000 days it can be seen that the 8 μm energy emitted by SN 2002hh was about 6 times greater. We also recall that the subtracted-image fluxes probably only represent lower limits for the amount by which the SN 2002hh mid-IR flux finally declined. The size of this decline is estimated in § 4.2 using an IR echo model, and we plan to measure this directly via later-epoch mid-IR images from *Spitzer*. These points argue against radioactively heated ejecta dust as the main source of the declining component.

Reverse-shock heating of ejecta dust is also unlikely, since, as late as 397 days, there was no evidence in the SN 2002hh optical spectra (Pozzo et al. 2006) of strong ejecta/CSM interaction as was seen, for example, in the Type IIn SN 1998S (Pozzo et al. 2004). Moreover, in optical spectra of SN 2002hh covering the period 650–1050 days (Clayton & Welch 2005) there is no sign of blueshifts in the Hα line profiles such as those that might have occurred if ejecta dust condensation had taken place. We conclude that IR emission from newly formed ejecta dust is unlikely to be the main cause of the declining component, whether heated by radioactivity or a reverse shock from a CSM impact.

4.2. *Mid-IR Emission from an IR Echo*

The total late-time mid-IR flux from the region of SN 2002hh could have been due to thermal emission from nearby dust following heating by supernova radiation emitted around the time of maximum light, i.e., an IR echo. Pozzo et al. (2006) have presented evidence from ground-based observations during the first year that a dusty CSM existed around SN 2002hh. Owing to the light-travel time across the dust region, the IR echo emission seen at Earth at a given time originates from a shell bounded by ellipsoidal surfaces, with the axis coincident with the line of sight. The thickness of this zone is fixed by the characteristic width of the SN bolometric light curve, which is dominated by UV-optical radiation. In addition, the peak light will evaporate dust out to a certain distance. Dwek (1983, 1985) has shown that for a supernova with a peak UV-optical luminosity of 1×10^{10} $L_\odot$ and an exponential decline rate timescale of 25 days, the dust-free cavity radius is about 6×10^{16} cm for carbon-rich (graphite) grains ($T_{\rm evap} = 1900$ K) and 3×10^{17} cm for oxygen-rich (silicate) grains ($T_{\rm evap} = 1500$ K). This is for 0.1 μm radius particles. Scaling to SN 2002hh using the early-time UV-optical light curve of Pozzo et al. (2006; see below), we infer a dust-free cavity of radius 2.6×10^{16} and 1.3×10^{17} cm for graphite and silicate grains, respectively. While the UV-optical ellipsoidal shell is still partially within the dust-free cavity, the IR light curve should be characteristically flat (Dwek 1983; Graham & Meikle 1986; Gerardy et al. 2002). This is due to the combined effects of the grain equilibrium temperatures, the cloud geometry, and the width and propagation of the ellipsoidal IR emission region. However, once the whole ellipsoidal shell has left the cavity, the IR flux declines.

We have constructed a simple IR echo model to test the possibility that the total mid-IR flux within the 3.″3 radius aperture originates in CSM dust heated by the peak SN luminosity. (Molecular cloud dust is discussed below.) In particular, we sought the lowest CSM dust mass that could provide the observed flux. The IR echo model follows those of Bode & Evans (1980), Dwek (1983), and Graham & Meikle (1986). The model assumes a spherically symmetric dust cloud having a single grain size, with the actual value of the grain radius as a free parameter. However, we have also explored the effect of a dust size distribution; this is briefly described below. Following Pozzo et al. (2006), the input UV-optical luminosity is a parameterized version of the peak and plateau parts of the SN 1999em *UBVRI* light curve (Elmhamdi

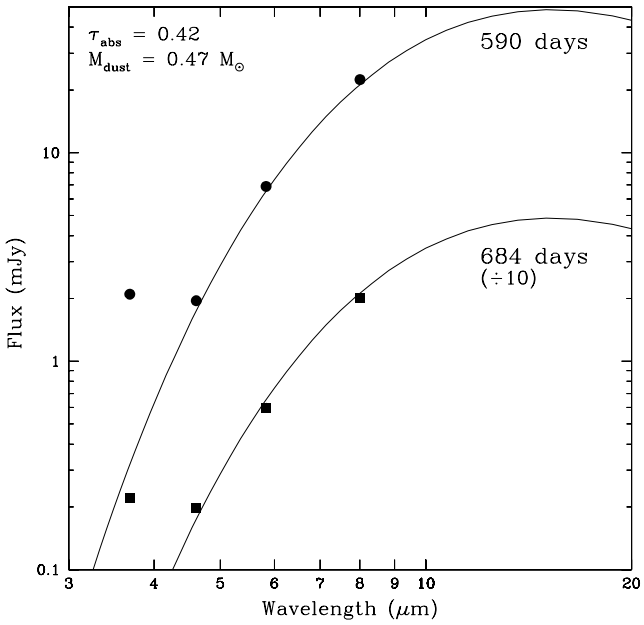

FIG. 7.—Dereddened SED of the SN 2002hh region (from unsubtracted images) at 590 days (*circles*) and 684 days (*squares*). Each point has been dereddened according to the two-component extinction of Pozzo et al. (2006), extrapolated to the mid-IR using the Cardelli et al. (1989) law. The individual points are located at the effective wavelengths of the IRAC filters for a 325 K blackbody. The 684 day fluxes are shown divided by 10 for clarity. The curves are synthetic spectra produced by an IR echo model with a dust mass of 0.47 $M_\odot$ [i.e., a CSM mass of $47(0.01/r_{dg})\ M_\odot$].

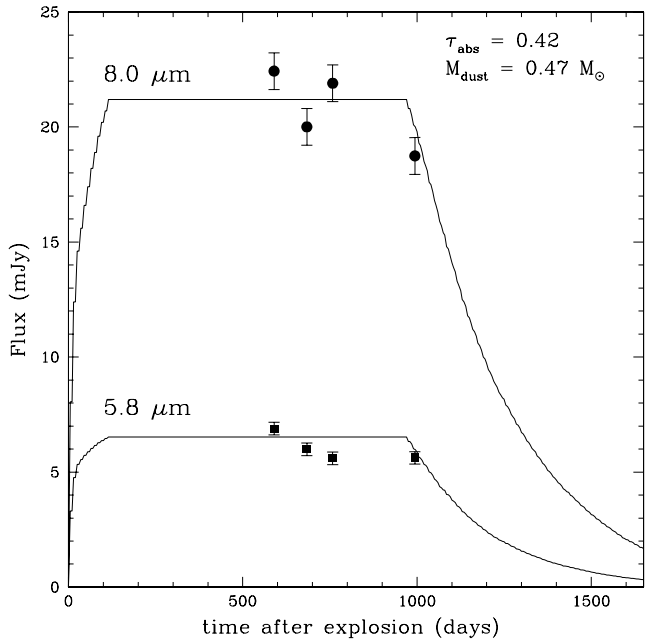

FIG. 8.—Dereddened 5.8 μm and 8.0 μm photometry of the SN 2002hh region (from unsubtracted images) compared with synthetic light curves produced by an IR echo model with a dust mass of 0.47 $M_\odot$ [i.e., a CSM mass of $47(0.01/r_{dg})\ M_\odot$]. The dust temperature at the inner boundary was 345 K during the IR echo plateau phase.

et al. 2003) corrected to the SN 1999em Cepheid distance of 11.7 Mpc (Leonard et al. 2003) and then scaled to the 5.9 Mpc distance of SN 2002hh. To allow for radiation shortward of the *U* band, we assumed that the supernova spectrum could be roughly described by a blackbody at 12,000 K during the peak, and 5500 K during the plateau. Therefore, we scaled the adopted light curve by 1.9 times in the peak and 1.05 times in the plateau. (For modest changes [$\Delta T \sim 1000$ K] in the adopted supernova peak temperature the derived dust mass varies roughly inversely with the temperature.) At wavelengths longer than the *I* band the fractions of the total blackbody radiation are about 5% at 12,000 K and 30% at 5500 K. However, at these wavelengths the absorptivity of the dust grains (size $\sim$0.1 μm) is likely to have fallen well below unity. Therefore, to simplify the IR echo calculation, we ignored the IR contribution to the total SN luminosity. We also ignored the radioactive tail since this is (1) much fainter than the earlier phases (<10% of the peak flux) and (2) dominated by IR radiation. Thus, the input UV-optical light curve used for the model is $47.0 \times 10^{41} e^{-t(d)/18.7}$ ergs s^{-1} for 24 days and $11.1 \times 10^{41} e^{-t(d)/171}$ ergs s^{-1} for 24–118 days. A grain material density of 3 g cm^{-3} was assumed. Given the typical grain size ($\sim$0.1 μm) required to reproduce the SED and still maintain a minimal dust mass, it is possible that, as for the near-IR, the absorptivity was below unity over at least part of the optical range of the SN peak luminosity spectrum. Therefore, for simplicity we adopted a single grain absorptivity to the input UV/optical light but allowed it to take values below unity. In calculating the mid-IR emission from the dust, for wavelengths longer than $2\pi a$, grain emissivities proportional to λ^{-1} and λ^{-2} were considered. Cloud density laws of r^{-1} and r^{-2} were used. To estimate the mass of associated circumstellar gas one can use the dust-to-gas mass ratio of the CSM. However, there is a wide range of values found for evolved massive stars; for example, Heras & Honey (2005) quote a range of 0.001–0.035 for oxygen-rich AGB stars. In view of this uncertainty, CSM mass estimates will be expressed in terms of the dust-to-gas mass ratio r_{dg} scaled to the typical ISM value of 0.01.

To reproduce the very slow observed decline in the total mid-IR flux (Fig. 3), it is necessary for the vertex of the outer echo ellipsoid to remain within a dust-free cavity for a time $t/2$, where t is the time to the latest observation (994 days). This corresponds to a cavity size of $ct/2 = 1.3 \times 10^{18}$ cm. As indicated above, the maximum likely size of an evaporated dust-free cavity would be only $\sim 1.3 \times 10^{17}$ cm. Thus, the only way in which a CSM cavity of the required size could occur would be via episodic mass loss. We adjusted the cavity radius to provide the best match to the light curve. This was obtained with an inner radius of 1.25×10^{18} cm. The outer radius was set at 2 times this value, although this is fairly uncritical. For a given combination of emissivity and density law, the grain size and emissivity were varied until the model SED matched that of the observed 4.5–8.0 μm fluxes. The 3.6 μm flux showed a large excess with respect to the model. As suggested above, most of this emission is probably due to a combination of nebular emission from the ejecta plus residual stellar/nebular background. The grain number density was then adjusted to match the total observed fluxes. With a λ^{-1} emissivity and a r^{-2} (steady wind) density law, a fair match to the data could only be achieved by increasing the dust mass to 0.47 $M_\odot$. This corresponds to a cloud mass of $47(0.01/r_{dg})\ M_\odot$, where r_{dg} is the dust-to-gas mass ratio. The grain radius was 0.15 μm and absorptivity was 1. This yielded a dust temperature at the inner boundary of 345 K during the echo-plateau phase, and a UV-optical absorption optical depth to the input SN luminosity of $\tau_{abs} = 0.42$. Use of a shallower density gradient or steeper emissivity law tended to increase the dust mass. The model matches to the 590 and 684 day SEDs and to the 5.8 and 8.0 μm light curves are shown in Figures 7 and 8, respectively. Even if we invoke a CSM dust-to-gas ratio toward the extreme high end of the observed range, the CSM mass would still be too large to have arisen from a progenitor mass-loss phase. We conclude that the *total* mid-IR emission within the 3.″3 radius aperture could not have arisen from an IR echo within

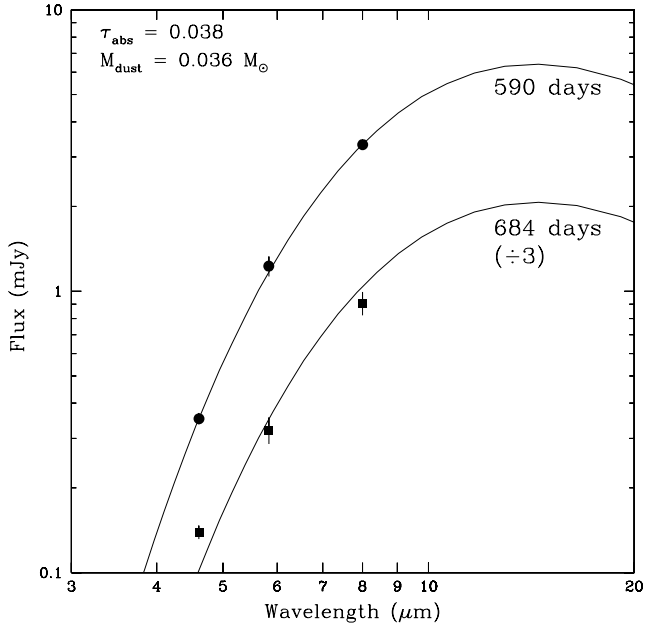

FIG. 9.—Dereddened SED of SN 2002hh (from subtracted images) at 590 days (*circles*) and 684 days (*squares*). Each point has been dereddened according to the two-component extinction of Pozzo et al. (2006), extrapolated to the mid-IR using the Cardelli et al. (1989) law. The individual points are located at the effective wavelengths of the IRAC filters for a 325 K blackbody. The zero-flux level of the data has been adjusted to optimize the match to the model light-curve shape (Fig. 10). The 684 day fluxes are shown divided by 3 for clarity. The curves are synthetic spectra produced by an IR echo model with a dust mass of 0.036 $M_\odot$ [i.e., a CSM mass of $3.6(0.01/r_{dg})$ $M_\odot$]. The dust temperature at the outer ellipsoid vertex declined from 375 K the end of the IR echo plateau phase, to 315 K by 1000 days.

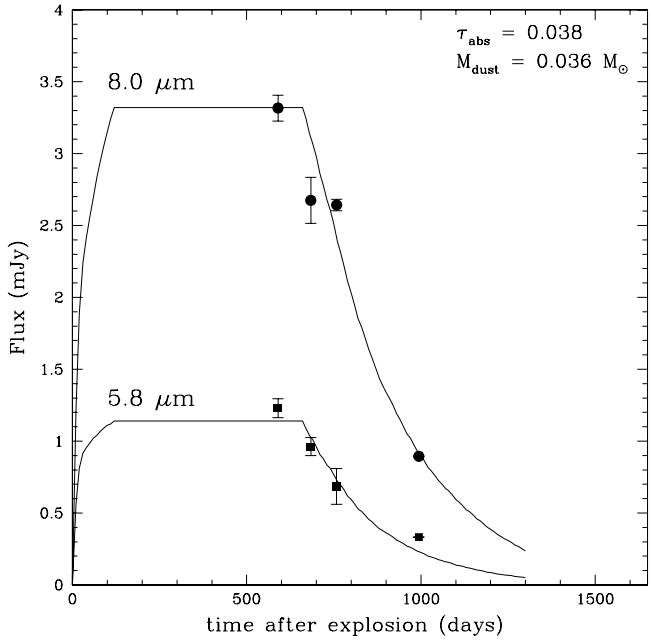

FIG. 10.—Dereddened 5.8 μm (*squares*) and 8 μm (*circles*) photometry of SN 2002hh (from subtracted images), compared with synthetic light curves produced by an IR echo model with a dust mass of 0.036 $M_\odot$ [i.e., a CSM mass of $3.6(0.01/r_{dg})$ $M_\odot$]. The zero-flux level of the data has been adjusted to optimize the match to the model light-curve shape.

a progenitor CSM. At this stage the possibility remains that most of the flux might have arisen from an IR echo from dust in a surrounding molecular cloud. This is addressed in § 4.4.

While we have concluded that the bulk of the mid-IR emission was not caused by a CSM-IR echo, it is still possible that it was responsible for a small part of the emission, specifically the declining component. We therefore repeated our CSM-IR echo analysis but this time using the supernova fluxes from the subtracted images (Table 4). Naturally, a much lower dust mass is required to reproduce the observations. As before, we endeavored to find the parameters that would minimize the mass of dust required. In particular, we increased the dust-free cavity radius and hence the plateau phase of the IR echo light curve as far as was compatible with the data. An additional free parameter was introduced to take into account the likelihood that the decline of the flux did not cease at 994 days. The zero-flux level of the data was therefore allowed to vary to optimize the match to the model light-curve shape. Good matches to the data were obtained with a grain radius of 0.07 μm and UV/optical absorptivity of 0.3. However, the dust mass is relatively insensitive to the choice of grain size/absorptivity parameter pair. The UV-optical absorption optical depth to the input SN luminosity was $\tau_{abs} = 0.038$. Thus, most of the extinction of the SN light must have occurred beyond the CSM. The outer and inner radii of the dust distribution are 0.86×10^{18} and 2.0×10^{18} cm, respectively. However, the outer radius is relatively uncritical for the match to the data. A lower value would reduce the dust mass, and vice versa. Other parameters were the same as those for the total-flux model. In Figure 9 we show the IR echo model matches to the observed SED at 590 and 684 days. In Figure 10 the IR-model light curves are compared with the observed evolution at 5.8 and 8.0 μm. The light-curve matches indicate that, between 590 and 994 days, the SN flux declined by ~0.75 of its 590 day value; i.e., by 994 days we estimate that the flux from the echo was about 0.3 mJy at 5.8 μm and 0.9 mJy at 8.0 μm. As mentioned earlier, we plan to measure the post-994 day evolution directly via later-epoch mid-IR images from *Spitzer*. We infer a dust mass of 0.036 $M_\odot$, corresponding to a CSM mass of $3.6(0.01/r_{dg})$ $M_\odot$. This gives a plausible CSM mass for a range of possible dust-to-gas ratios. The large radius of the inner boundary of the dust required to minimize the dust mass means that it is necessary to invoke episodic mass loss. For a wind velocity of 10 km s^{-1} the radius implies that the mass-loss phase declined significantly about 28,000 years before the supernova explosion. This timescale can be reduced but at the cost of increasing the dust mass. The key point is that the declining component *can* be reproduced using an IR echo from a CSM of just a few solar masses. However, if the supernova was embedded in a molecular cloud, an alternative scenario is that the declining flux was due to an IR echo from dense ISM dust in the supernova vicinity.

The above modeling was based on the assumption of a single grain size. It may be argued that a more realistic approach is to use a plausible grain size distribution. We have explored the effect of introducing into the IR echo model a grain size distribution $dn \propto a^{-3.5} da$ with 0.005 μm $< a <$ 0.25 μm (Mathis et al. 1977). A grain emission/absorption efficiency proportional to λ^{-1} was adopted when $\lambda > 2\pi a$, and constant otherwise. We find very similar results to those obtained with the single grain size assumption. The derived dust masses were about 5%–10% lower than those in the single-sized grain case.

4.3. *Mid-IR Emission from Ejecta/CSM Interaction*

We have also considered the possibility that the total mid-IR luminosity was due to the impact of the ejecta on a dusty CSM. As increasing amounts of ejecta gradually encountered the CSM dust, the relatively constant mid-IR flux might be produced. However, for this to work, the dust-free cavity evaporated by the

peak luminosity must not be so large that the ejecta could not have reached the surviving dust by the beginning of the observations. As explained above, we estimate a dust-free cavity of radius between 2.6×10^{16} and 1.3×10^{17} cm. However, the lower limit is somewhat irrelevant here, since to provide the total observed SED at 590 days would require a blackbody of radius 9×10^{16} cm (see above). As already indicated, to reach a distance of 9×10^{16} cm in just 590 days would take a velocity of $\sim$18,000 km s^{-1}. For a dust-free cavity of radius 1.3×10^{17} cm it would require 26,000 km s^{-1}. Inclusion of light-travel time effects would increase these velocities by a further 5%–10%. Only the very fastest, outermost material is likely to be moving with such velocities. It is unlikely that sufficient energy could be transferred to the CSM dust by such tenuous material to account for the 590 day luminosity. Moreover, to explain the observed mid-IR flux and SED the dust would have to be optically thick *in the mid-IR region* or at least close to being so. For an optical depth of unity at $\sim$8 μm, the two-component extinction scenario derived by Pozzo et al. (2006) extrapolated to the V band using Cardelli et al. (1989) indicates an $A_V \sim 90$. Even if we adopt the flatter λ^{-1} dependence used in our IR echo model, the V-band extinction would be at least $A_V = 15$. Yet Pozzo et al. (2006) observe only $A_V = 5.0$. Moreover, they find that K I absorption suggests that at least $A_V \sim 3$ of this is probably interstellar extinction in the host galaxy and Milky Way. We conclude that the total mid-IR emission is unlikely to be due to ejecta impact onto CSM dust or, indeed, onto ISM dust.

We have also considered the possibility that just the declining component of the mid-IR emission was due to ejecta/CSM impact. As shown above, to reproduce the 590 day declining-component emission the minimum source size corresponds to a blackbody expanding at 4800 km s^{-1}. This is equivalent to a radius of 2.4×10^{16} cm, which is only just below the minimum grain survival radius of 2.6×10^{16} cm (see above). Given that higher ejecta velocities exist, could it be that an ejecta/CSM impact is a plausible alternative to an IR echo mechanism? To address this question, suppose that to find enough ejecta kinetic energy to power the mid-IR flux we must include all velocities down to 10,000 km s^{-1}; i.e., we consider ejecta/CSM impact heating of dust lying at roughly twice the above blackbody radius. Let us assume that the emission from the dust is proportional to $(1 - e^{-\tau}) r_{\rm dust}^2$, where τ is the optical depth and $r_{\rm dust}$ is the dust cloud inner radius. If we assume that the "blackbody" optical depth at 8 μm is at least 2, then for dust at 10,000 km s^{-1} to produce the observed 8 μm emission we would require an optical depth of about 0.25. Adopting a conservative λ^{-1} dependence of the grain absorption/emission efficiency, this implies an $A_V \sim 4.0$. This is still substantially larger than the extinction that Pozzo et al. (2006) attribute to dust local to the supernova. Moreover, as noted above (§ 4.1), in optical spectra of SN 2002hh covering the period 650–1050 days (Clayton & Welch 2005) there is no sign of blueshifts in the Hα line profiles such as those that might have occurred if optically thick dust were present. Also, as noted earlier, as late as 397 days there was no evidence in the SN 2002hh optical spectra (Pozzo et al. 2006) of strong ejecta/CSM interaction. Another possible problem is that, given the increasing amounts of ejecta moving into the dust, it might be difficult to account for the apparently quite rapid decline ($\sim$0.42 mag per 100 days) in the mid-IR light curve (Fig. 10). We conclude that, while not ruled out completely, it seems unlikely that ejecta/CSM impact can account for most of the declining mid-IR emission.

In spite of the above conclusions, we know from the radio observations of Beswick et al. (2005) that some interaction between the ejecta and circumstellar material was taking place as late as 899 days. In addition, we have acquired near-IR evidence for a late-time CSM/ejecta impact. We used the TIFKAM IR imager at the 2.4 m telescope of the MDM Observatory, Kitt Peak, to obtain deep *JHK* images of the SN 2002hh field at 926 days. In all three bands we see a weak but clearly detected point source within 0.″15 of the supernova position. After dereddening, the IR fluxes are 0.18, 0.11, and 0.18 mJy at *J*, *H*, and *K*, respectively, with an uncertainty of $\pm$0.01 mJy in each band. We have searched for this source in preexplosion images. Unfortunately, there are no *JHK* images of equivalent depth and resolution. However, a deep $i_{\rm CCD}$-band image taken under fair seeing conditions (S. Smartt 2006, private communication) shows no point source at the supernova location, with a 5 σ limit of 22.3. This translates to a dereddened limit of 0.015 mJy. We suggest, therefore, that the *JH* emission was produced by the supernova (the origin of the *K* flux is discussed below). These fluxes are over 100 times greater than the *JH* flux from SN 1987A (scaled to 5.9 Mpc) at the same epoch. Indeed, the *JH* point source luminosity exceeds the total likely radioactive deposition (Li et al. 1993) by a factor of 10. We therefore eliminate radioactively driven ejecta emission as the source of the *JH* luminosity. The dereddened $J - H$ is about zero, suggesting a characteristic temperature of around 10,000 K. This rules out an IR echo source since the dust temperature is too high. We therefore suggest that the *JH* flux is due to ejecta/CSM interaction. Indeed, a blackbody at this temperature would only need a velocity of $\sim$5 km s^{-1} to produce the observed *JH* flux. For the excess *K*-band emission, we think a supernova origin is less likely. Extrapolation of the 18,000 km s^{-1} blackbody (see § 4.1) to the *K* band, with a slightly higher temperature of $\sim$400 K, shows that much of the *K* excess could simply be due to the Wien tail of the cool mid-IR source.

4.4. *On the Nature of the Mid-IR Source at the SN 2002hh Location*

To explore further the origin of the bulk of the mid-IR flux, we have compared the *Spitzer* 590 day 8 μm image with preexplosion *ISO* images of the same field (Roussel et al. 2001). In Figure 11 we show the 8 μm (bandpass = 6.4–9.3 μm) *Spitzer* image placed between the 7 μm (bandpass = 5.0–8.5 μm) and 15 μm (bandpass = 12.0–18.0 μm) *ISO* images. We have rebinned and smoothed the 8 μm image to match the $\sim$6″ resolution of the *ISO* images. The contrast levels were set so that the galaxy structure features are of similar contrast in each image. Further details are given in the figure legend. As we go from short to long wavelengths, the 2MASS star steadily fades as expected for a hot object. It dominates the supernova field at 7 μm but is less prominent at 8 μm. By 15 μm the star is actually slightly fainter than a source lying about 6″ (2 pixels) east and 3″ (1 pixel) south of it; i.e., the images appear to be consistent with an almost unvarying cool source lying to the east and south of the 2MASS star, close to the supernova location. Extrapolation from the 8 μm image to 7 μm assuming a Rayleigh-Jeans slope for the 2MASS star spectrum and a 320 K blackbody for the cool source (§ 4.1) yields a total flux for the 2MASS star + cool source that can be directly compared with that measured in the 7 μm preexplosion *ISO* image. Allowing for the uncertainties in this extrapolation, we deduce that less than half of the flux from the cool 8 μm source can be due to the supernova explosion. This suggests that *most* of the mid-IR flux from the supernova direction was not actually due to the supernova; i.e., most of the flux was not due to an IR echo from the CSM, supporting the conclusions from our IR echo modeling above, nor was it due to an IR echo from a surrounding dusty molecular cloud. The *Spitzer* images show that the region around the supernova is rich in cool, mid-IR emitting structures (cf. Fig. 1),

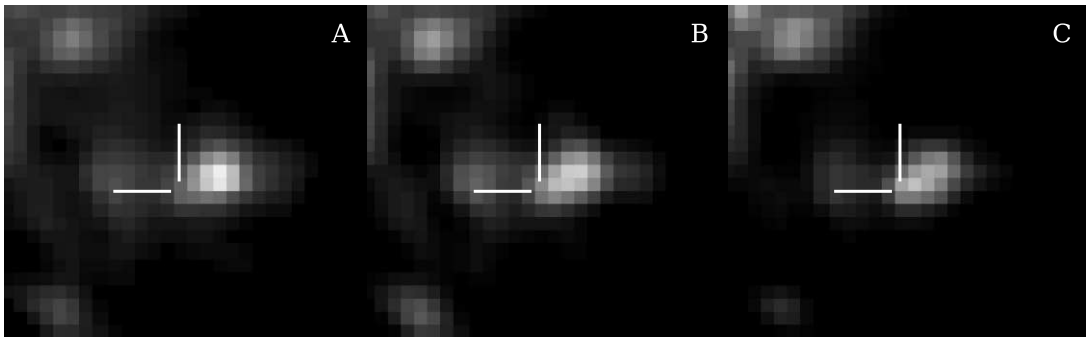

FIG. 11.—Comparison of the 590 day 8 μm *Spitzer* image of the (B) SN 2002hh field with preexplosion *ISO* images (from Roussel et al. 2001) of the same field at (A) 7 μm and (C) 15 μm, respectively. The image FOV of each image is $82'' \times 76''$. North is up, and east is to the left. The pixel size is $3''$. The SN location is marked with ticks in each image. The 2MASS star lies about $9''$ from the supernova location at P.A. 298°. As we go from short to long wavelengths, the 2MASS star steadily fades, as expected for a hot object. By 15 μm the star is slightly fainter than a source lying about $6''$ east and $3''$ south of it; i.e., the images appear to be consistent with an almost unvarying cool source lying to the east and south of the 2MASS star, close to the supernova location. To prepare this figure, the *ISO* 7 μm image was first rotated to align the pixel and northeast axes. The *Spitzer* image was then aligned and rebinned to match the 7 μm image. The aligned *Spitzer* image was then smoothed with a Gaussian kernel with sigma = 1 pixel, to match the *ISO* resolution. Finally, the 15 μm *ISO* frame was rotated and shifted to match the aligned *Spitzer* frame using the positions of three sources around the SN, including the blend between the 2MASS star and the nearby cool source.

and we suggest that such a source lying close to the line of sight is responsible for most of the observed mid-IR flux. We propose that a luminous but highly obscured object, such as a star formation region and/or molecular cloud could be responsible. If the supernova lies behind or is embedded in this cloud, it could explain the high extinction. In particular, it may account for the anomalous extinction component identified by Pozzo et al. (2006). In addition, as suggested above (§ 4.2), such a cloud may also have produced the declining component of the mid-IR flux via an IR echo.

Comparison of the *Spitzer* 3.6 μm flux with the earlier L'-band evolution (Pozzo et al. 2006) supports our contention that most of the flux in the unsubtracted images was not due to the supernova. Simple extrapolation of the L'-band light curve to 590 days predicts a flux of 0.19 mJy. This is nicely consistent with the 0.2 mJy upper limit for the 3.6 μm subtracted images (Table 4) but is less than a tenth of the 2.5 mJy in the unsubtracted images.

4.5. *Comparison with the Work of the SEEDS Collaboration*

The SEEDS collaboration (Barlow et al. 2005) have also presented flux estimates for the SN 2002hh region in the SINGS images (see § 2), and we now compare their results with those presented here. They used a PSF fitting procedure to determine the fluxes. For both SINGS epochs, at 4.5 and 5.8 μm, their fluxes are typically ~65% of the values we obtained from the unsubtracted images. At 8 μm their fluxes are, respectively, about 80% and 60% of our values at 590 and 758 days. Given the complexity of the field and the different photometry techniques used, these differences are not surprising. Between 590 and 758 days we find that the 5.8 μm flux fell by about 0.14 ± 0.07 mJy, compared with a 0.63 ± 0.61 mJy decline reported by Barlow et al. (2005). While there appears to be a disagreement, the difference is actually only at the level of 0.8 σ when the large error in the latter value is taken into account. Similarly, at 8.0 μm we find the flux fell by 0.64 ± 0.10 mJy compared with 4.2 ± 2.1 mJy for Barlow et al. (2005). Here the disagreement seems even greater than at 5.8 μm, but again the large SEEDS error means that the significance is only 1.7 σ. Thus, there is actually fair consistency between the two sets of results. However, the present work indicates that, relative to the *total* flux, the 8.0 μm 590–758 day decline was only ~4% (scaled to the Barlow et al. total fluxes) and not 25% as adopted by Barlow et al. (2005).

Barlow et al. (2005) modeled the mid-IR flux using a dusty CSM heated by a "central source." While their measured fluxes are comparable to the values we obtain from the unsubtracted images, they infer a dust mass of 0.10–0.15 $M_\odot$, i.e., a factor of ~4 less than our 0.47 $M_\odot$ dust mass estimate based on the total fluxes. A possible reason for the large discrepancy between our respective estimates is their apparent noninclusion of light-travel time effects in their models. One consequence of light-travel time delays is that, at any given time, the bulk of the IR flux we receive may come from only a relatively small fraction of the CSM, bounded by the echo ellipsoids corresponding to the characteristic width of the early-time light curve. We therefore suggest that, assuming a spherically symmetric CSM, Barlow et al. have underestimated the CSM mass required to reproduce the total observed mid-IR flux via this mechanism. In addition, we note that the Barlow et al. (2005) inner CSM radius of only 2.1×10^{17} cm (~80 lt-days) in their best-fitting model is unlikely to reproduce the near-constant flux to 994 days. Barlow et al. also present an 11.2 μm image of the supernova field obtained at the 8 m Gemini North telescope at 698 days. The spatial resolution is $0''.3$ (8.6 pc at NGC 6946)—considerably higher than that of *Spitzer*. A bright unresolved point source is apparent at the supernova location, which they identify with the supernova. However, as argued above, we believe that the bulk of the mid-IR flux in this wavelength region is not from the supernova but rather is due to a luminous, obscured star formation region or molecular cloud. It is our view that most of the flux assumed by Barlow et al. (2005) to have been driven by the supernova was, in fact, from a separate, causally unconnected source.

5. SUMMARY

We have presented late-time mid-IR observations of the normal but highly reddened Type IIP SN 2002hh. This is only the second-ever core-collapse supernova to be observed at such late epochs in the mid-IR and is the first Type IIP to be studied in this way. The 4.5–8.0 μm flux from within $3''.3$ (~100 pc) of the supernova reveals bright, cool emission with a characteristic temperature of about 320 K. A flux decline of about 10% was seen between 590 and 994 days. We rule out condensing dust in the ejecta, an ejecta/CSM impact, or a CSM-IR echo as the cause of most of the observed mid-IR flux. Comparison of the *Spitzer* data with preexplosion *ISO* images also tends to rule out an IR echo from ISM dust. This comparison suggests, rather, that most of

the mid-IR flux from the supernova direction is actually due to a luminous, cool source such as a heavily obscured star formation region or molecular cloud lying along the line of sight. This is supported by extrapolation of the L'-band light curve. The supernova may actually lie behind or be embedded in the obscured source, which would account for the high extinction observed. We disagree with Barlow et al. (2005) that most of the mid-IR flux is due to the supernova and with their suggestion that a large fraction of the extinction to SN 2002hh appears to be due to CS dust.

We assume that the small declining component of the mid-IR flux was powered by SN 2002hh. As possible sources we considered (1) newly condensed dust in the ejecta, (2) an IR echo from a dusty CSM, and (3) ejecta/dusty CSM impact. Of these, an IR echo provides the most plausible explanation for most of the declining component. If the supernova was embedded in the molecular cloud, then it is possible that the IR echo was from dense ISM dust rather than from the progenitor CSM. Emission from condensing ejecta dust contributes, at most, a small fraction of the declining flux. This appears to be consistent with the absence of late-time blueshifts in the Hα line profiles (Clayton & Welch 2005). However, it may be that a substantial mass of dust formed in the ejecta but is largely concealed in optically thick regions. A similar point has been made by Barlow et al. (2005). Emission from CSM dust heated in an ejecta/CSM impact is not completely ruled out, but given the difficulties in reconciling this with the observed optical extinction, the Clayton & Welch (2005) result, and, perhaps, the rapid decline of the mid-IR flux, it seems that this mechanism also can only provide a small part of the declining mid-IR flux.

We conclude that SN 2002hh produced an IR echo from dust, either in the progenitor CSM or in a surrounding molecular cloud, and that this was responsible for most of the declining component of the mid-IR flux. For the CSM scenario, we deduce that the mid-IR flux could have been produced by a dust mass of as little as 0.036 $M_\odot$ lying between 0.86×10^{18} and 2.0×10^{18} cm from the SN. The corresponding CSM mass is $3.6(0.01/r_{\rm dg})\ M_\odot$. This gives a plausible CSM mass for a range of possible dust-to-gas ratios. To account for the large inner boundary radius it is necessary to invoke episodic mass loss. For a wind velocity of 10 km s^{-1}, this radius implies that the mass-loss rate declined sharply around 28,000 years before the explosion. Pozzo et al. (2006) used near-IR observations of SN 2002hh during the first year to deduce a dusty CSM mass of just 0.3 $M_\odot$, with an inner boundary at 1.3×10^{17} cm. However, this does not necessarily conflict with our mid-IR result as the Pozzo et al. (2006) study was sensitive only to hot dust ($T \sim 1000$ K) lying close to the supernova. Such dust could have formed in a much reduced mass-loss phase that took place after the main mass-loss phase ended 28,000 years ago. The small amount of hot dust detected by Pozzo et al. (2006) would have been undetectable by our *Spitzer* study. In addition, Pozzo et al. (2006) would have been unable to detect the large CSM mass reported here as it was too cold. This scenario is consistent with the weak CSM interaction inferred at early times by Pooley & Lewin (2002) and Stockdale et al. (2002), and the low mass-loss rate deduced from the early-time radio observations by Chevalier et al. (2006). This ongoing ejecta/CSM collision could also account for the very late time *JH*-band source at the supernova position. The preexplosion i' band image (§ 4.3) allows an upper limit of 20 $M_\odot$ to be placed on the progenitor mass (S. Smartt 2006, private communication). A star of mass just below this limit could plausibly lose 3–10 $M_\odot$ during its red supergiant phase, consistent with the $3.6(0.01/r_{\rm dg})\ M_\odot$ CSM deduced from the IR echo analysis. For the molecular cloud IR echo case, it is likely that a similar mass would have been involved in producing the IR radiation, but this could be just a small fraction of the total mass in the cloud. Our IR echo analysis was based on the assumption of a spherically symmetric dust cloud, and we have shown that this was sufficient to account for the mid-IR fluxes and evolution. Consequently, asymmetric dust distributions (Emmering & Chevalier 1988) were not considered on this occasion.

This work demonstrates for the first time that an IR echo has occurred in an apparently normal Type IIP supernova, the commonest of all supernovae. We find no evidence for or against the proposition that ejecta dust formation in such supernovae produces the 0.1–1 $M_\odot$ of grains required if such events are to be established as a major contributor to the dust content of the universe. However, substantial masses of newly condensed grains may lie concealed in optically thick regions. Observations carried out at later epochs and longer wavelengths should allow us to decide if this is the case. If we opt for a CSM-IR echo, the $\sim$0.04 $M_\odot$ of dust in the progenitor wind is considerably larger than the $\sim 10^{-3}\ M_\odot$ of directly observed ejecta dust that has been deduced from studies of SNe 1987A, 1998S, and 1999em. Thus, while we cannot yet decide if Type IIP supernovae form large masses of grains, it does appear that important contributions to the dust content of the present universe could be made by their progenitor winds.

We thank Christophe Alard for helpful discussions, Steve Smartt for his progenitor mass limit estimate, and Mike Barlow for a computer readable version of the 11.2 μm image of the SN 2002hh field. C. L. G. was supported in part by PPARC grant PPA/G/S /2003/00040. R. K. was supported in part by EU RTN grant HPRN-CT-2002-00303. S. M. acknowledges financial support from the European Science Foundation. M. P. is supported by PPARC grant PPA/G/S/2001/00512. J. C. W. is supported in part by NSF grant AST 04-06740. This work is based on observations made with the *Spitzer Space Telescope*, which is operated by the Jet Propulsion Laboratory, California Institute of Technology under a contract with NASA. Support for this work was provided by NASA through an award issued by JPL/Caltech.

Facility: Spitzer

REFERENCES

Alard, C. 2000, A&AS, 144, 363
Alard, C., & Lupton, R. H. 1998, ApJ, 503, 325
Barlow, M. J., et al. 2005, ApJ, 627, L113
Bertoldi, F., Carilli, C. L., Cox, P., Fan, X., Strauss, M. A., Beelen, A., Omont, A., & Zylka, R. 2003, A&A, 406, L55
Beswick, R. J., Fenech, D., Thrall, H., Argo, M. K., Muxlow, T. W. B., & Pedlar, A. 2005, IAU Circ. 8572
Bode, M. F., & Evans, A. 1980, MNRAS, 193, 21P
Bouchet, P., & Danziger, I. J. 1993, A&A, 273, 451
Cardelli, J. A., Clayton, G. C., & Mathis, J. S. 1989, ApJ, 345, 245
Cernuschi, F., Marsicano, F., & Codina, S. 1967, Ann. d'Astrophys., 30, 1039
Chandra, P., Ray, A., & Bhatnagar, S. 2003, IAU Circ. 8041
Chevalier, R. A., Fransson, C., & Nymark, T. K. 2006, ApJ, 641, 1029
Clayton, D. D., Amari, S., & Zinner, E. 1997, Ap&SS, 251, 355
Clayton, G. C., & Welch, D. L. 2005, BAAS, 37, 1433
Danziger, I. J., Lucy, L. B., Bouchet, P., & Gouiffes, C. 1989, Supernovae: The Tenth Santa Cruz Workshop in Astronomy and Astrophysics, ed. S. E. Woosley (New York: Springer), 69
Douvion, T., Lagage, P. O., & Pantin, E. 2001, A&A, 369, 589
Draine, B. T. 2003, ARA&A, 41, 241
Draper, P. W., Gray, N., & Berry, D. S. 2004, Starlink User Note 214.10 (Suindoni: PPARC), http://www.starlink.ac.uk/cgi-bin/hcserver?sun214.15

Dunne, L., Eales, S., Ivison, R., Morgan, H., & Edmunds, M. 2003, Nature, 424, 285
Dwek, E. 1983, ApJ, 274, 175
———. 1985, ApJ, 297, 719
———. 2004, ApJ, 607, 848
Dwek, E., Dinerstein, H. L., Gillett, F. C., Hauser, M. G., & Rice, W. L. 1987, ApJ, 315, 571
Dwek, E., Moseley, S. H., Glaccum, W., Graham, J. R., Loewenstein, R. F., Silverberg, R. F., & Smith, R. K. 1992, ApJ, 389, L21
Elmhamdi, A., et al. 2003, MNRAS, 338, 939
Emmering, R. T., & Chevalier, R. A. 1988, AJ, 95, 152
Fall, S. M., Charlot, S., & Pei, Y. C. 1996, ApJ, 464, L43
Fall, S. M., Pei, Y. C., McMahon, R. G. 1989, ApJ, 341, L5
Fazio, G., et al. 2004, ApJS, 154, 10
Filippenko, A. V., Foley, R. J., & Swift, B. 2002, IAU Circ. 8007
Fransson, C., & Chevalier, R. A. 1987, ApJ, 322, L15
Gerardy, C. L., et al. 2002, ApJ, 575, 1007
Graham, J. R., & Meikle, W. P. S. 1986, MNRAS, 221, 789
Heras, A. M., & Hony, S. 2005, A&A, 439, 171
Hoyle, F., & Wickramasinghe, N. C. 1970, Nature, 226, 62
Karachentsev, I. D., Sharina, M. E., & Huchtmeier, W. K. 2000, A&A, 362, 544
Kennicutt, R. C., Jr., et al. 2003, PASP, 115, 928
Knapen, J. H., Stedman, S., Bramich, D. M., Folkes, S. L., & Bradley, T. R. 2004, A&A, 426, 1135
Kotak, R., Meikle, W. P. S., Adamson, A., & Leggett, S. K. 2004, MNRAS, 354, L13
Krause, O., Birkmann, S. M., Rieke, G. H., Lemke, D., Klaas, U., Hines, D. C., & Gordon, K. D. 2004, Nature, 432, 596
Lagage, P. O., Claret, A., Ballet, J., Boulanger, F., Césarsky, C. J., Césarsky, D., Fransson, C., & Pollock, A. 1996, A&A, 315, L273
Larsen, S. S., & Richtler, T. 1999, A&A, 345, L59
Leonard, D. C., Kanbur, S. M., Ngeow, C.C, Tanvir, N. R. 2003, ApJ, 594, 247
Li, H., McCray, R., & Sunyaev, R. A. 1993, ApJ, 419, 824
Li, W. 2002, IAU Circ. 8005
Lucy, L. B., Danziger, I. J., Gouiffes, C., & Bouchet, P. 1991, Supernovae: The Tenth Santa Cruz Workshop in Astronomy and Astrophysics, ed. S. E. Woosley (New York: Springer), 82
Mathis, J. S., Rumpl, W., & Nordsieck, K. H. 1977, ApJ, 217, 425
Mattila, S., & Meikle, W. P. S. 2001, MNRAS, 324, 325
Meikle, P., Mattila, S., Smartt, S., MacDonald, E., & Clewley, L. 2002, IAU Circ. 8024
Meikle, W. P. S. 2005, BAAS, 37, 470
Meikle, W. P. S., Spyromilio, J., Allen, D. A., Varani, G.-F., & Cumming, R. J. 1993, MNRAS, 261, 535
Nozawa, T., Kozasa, T., Umeda, H., Maeda, K., & Nomoto, K. 2003, ApJ, 598, 785
Pei, Y. C., Fall, S. M., & Bechtold, J. 1991, ApJ, 378, 6
Pettini, M., King, D. L., Smith, L. J., & Hunstead, R. W. 1997, ApJ, 478, 536
Pooley, D., & Lewin, W. H. G. 2002, IAU Circ. 8024
Pozzo, M., Meikle, W. P. S., Fassia, A., Geballe, T., Lundqvist, P., Chugai, N. N., & Sollerman, J. 2004, MNRAS, 352, 457
Pozzo, M., Meikle, W. P. S., Rayner, J. T., Joseph, R. D., Filippenko, A. V., Foley, R. J., Li, W., Mattila, S., & Sollerman, J. 2006, MNRAS, 368, 1169
Reach, W. T., et al. 2006, Infrared Array Camera Data Handbook, Ver. 3.0 (Pasadena: Spitzer Science Center), http://ssc.spitzer.caltech.edu/irac/dh/iracdatahandbook3.0.pdf
Roche, P. F., Aitken, D. K., & Smith, C. H. 1993, MNRAS, 261, 522
Roussel, H., et al. 2001, A&A, 369, 473
Spyromilio, J., & Graham, J. R. 1992, MNRAS, 255, 671
Stockdale, C. J., et al. 2002, IAU Circ. 8018
Todini, P., & Ferrara, A. 2001, MNRAS, 325, 726
Whitelock, P. A., et al. 1989, MNRAS, 240, 7P
Wooden, D. H., Rank, D. M., Bregman, J. D., Witteborn, F. C., Tielens, A. G. G. M., Cohen, M., Pinto, P. A., & Axelrod, T. S. 1993, ApJS, 88, 477